Chemical Physics 380 (2011) 34–39

Contents lists available at ScienceDirect

Chemical Physics

journal homepage: www.elsevier.com/locate/chemphys

The structure and vibrational spectra of the 2,5-dimethylpyrazine (2,5-DMP) 1:1 adduct with 2,5-dichloro-3,6-dihydroxy-p-benzoquinone (CLA)

A. Pawlukojć [a], W. Sawka-Dobrowolska [b], G. Bator [b,*], L. Sobczyk [b], E. Grech [c], J. Nowicka-Scheibe [c]

[a] *Institute of Nuclear Chemistry and Technology, Dorodna 16, 03-195 Warsaw, Poland*
[b] *Faculty of Chemistry, University of Wrocław, F. Joliot-Curie, 1450 383 Wrocław, Poland*
[c] *Department of Inorganic and Analytical Chemistry, Westpomeranian University of Technology, Al. Piastów 42, 71-065 Szczecin, Poland*

ARTICLE INFO

Article history:
Received 1 March 2010
In final form 15 December 2010
Available online 22 December 2010

Keywords:
Hydrogen bonds
2,5-dimethylpyrazine
Chloranilic acid
Hadži's trio
Torsional modes of methyl groups
Inelastic neutron scattering

ABSTRACT

The complexation of 2,5-dimethylpyrazine (2,5-DMP) with 2,5-dichloro-3,6-dihydroxy-p-benzoquinone (CLA) leads to the formation of the hydrogen bonded OH···N infinite chains without any proton transfer. In the high and medium frequency region of the IR spectra a characteristic Hadži's trio with maxima at *ca.* 2400, 1800 and 1150 cm^{-1} is observed. The infrared, Raman and inelastic neutron scattering (INS) spectra are compared with those calculated by using the DFT methods applied to the crystalline state. The optimization of the structure by using this theoretical approach is also performed. Very good conformity of the experimental and theoretical structures is visible. The reproduction of vibrational spectra is also good except for the low frequency bands related to the CH_3 torsional modes. One gets relatively good agreement by using PWC(dnp) approach. Applications of other theoretical models leads to much higher values of CH_3 torsional frequency.

1. Introduction

Pyrazine and its derivatives merit being distinguished from the point of view of crystal engineering and material sciences [1–5]. The same is related to 2,5-dichloro-3,6-dihydroxy-p-benzoquinone (chloranilic acid – CLA) [6,7] and squaric acid (H_2SQ) [8], which possess two equivalent proton donor groups. Moreover CLA is interesting from a biological point of view as a benzoquinone derivative being an electron accepting system [9]. Both pyrazine and CLA and H_2SQ possess two centers with an ability to form bridges of the hydrogen bond (HB) or charge transfer (CT) type.

The methyl derivatives of pyrazine and particularly tetramethylpyrazine (TMP) in complexes with either CLA [10,11] or H_2SQ [12,13] have been the subject of particular interest. TMP with either p-nitrophenol [14] or picric acid [15] forms also an interesting complex of the 1:2 composition. In the former case the TMP molecule forms two hydrogen bonds without any proton transfer, while in the latter case the protonation of both nitrogen atoms takes place.

The complex of 2,6-dimethylpyrazine (26DMP) with chloranilic acid [16,17] has been the object of studies as well. The main result for this complex was the comparison of frequencies for the torsional modes of methyl group with those calculated for the crystalline state. Generally one observes a good agreement between the calculated and experimental frequencies of the vibrations. This observation is valid over a broad frequency range with the exception, however, of the CH_3 torsional modes. The calculated frequencies appeared to be much higher than the experimental ones. Therefore it seems justified to examine the adduct of 2,5-DMP with CLA, to prove generally this observation. In the present work we decided to synthesize the crystalline 2,5-DMP·CLA adduct in order to study the X-ray structure, which has been not known so far, as well as to analyze the vibrational spectra obtained from the complementary INS, infra-red and Raman techniques.

It should be noted that the infrared and Raman spectra at room temperature of the pure component of the 2,5-DMP·CLA adduct – 2,5-dimethylpyrazine have been already recorded and the energy levels of the methyl groups were obtained on the basis of a molecular geometry [18].

2. Experimental and calculations

The crystalline 1:1 adduct of 2,5-dimethylpyrazine (2,5-DMP) with 2,5-dichloro-3,6-dihydroxy-p-benzoquinone (CLA) was obtained by a slow evaporation of acetone as a solvent containing 1:1 mixture of components.

The X-ray diffraction studies were performed on a Kuma KM4 CCD *x*-axis four circle diffractometer equipped with an Oxford Cryosystem Cooler using graphite monochromated MoKα radiation. The data were corrected for Lorentz and polarization effects as well as for absorption.

---

* Corresponding author.
E-mail address: gb@wchuwr.chem.uni.wroc.pl (G. Bator).

0301-0104/$ - see front matter © 2011 Elsevier B.V. All rights reserved.
doi:10.1016/j.chemphys.2010.12.003

The structure was solved by direct methods (SHELXS-97) and refined by the full-matrix least-squares methods using the SHELXL-97 [19] program. Non-hydrogen atoms were refined with anisotropic thermal parameters. The hydrogen atoms attached to carbon were placed at calculated positions and refined. Allowing them to ride on the parent carbon atom. The hydrogen atom of O–H group was located from difference map and refined. The crystal data and structure refinement are summarized in Table 1. Crystallographic data for the structural analysis have been deposited with the Cambridge Crystallographic Data Centre, CCDC 767413.

Infra-red spectra of 2,5-DMP CLA crystal were recorded at room temperature with the FTIR spectrometer BRUKER IFS-113v over the wavenumber range 4000–40 cm^{-1} with a resolution of 1.0 cm^{-1}. For the mid-IR spectra the samples were studied as a suspension in Nujol or Fluorolube between the KBr windows. The far-IR spectra were taken in Nujol mulls between the polyethylene windows over the wavenumber range 600–50 cm^{-1}.

The Raman spectra of powder samples were recorded on a Nicolet Magna 860 FT Raman spectrometer at room temperature. Nd:YAG laser was the exciting source, with power of *ca.* 200 mW. The back scattering geometry was applied. The resolution was set up for 2 cm^{-1}.

Neutron scattering data were collected at the pulsed IBR-2 reactor in Dubna using the time-of-flight inverted geometry spectrometer NERA-PR [20] at 20 K. The spectra were converted from neutron per channel to $S(Q, \omega)$ scattering function per energy transfer. At the energy transfer between 5 and 100 meV the relative INS resolution was estimated to be *ca.* 3%.

The total energy optimization and the frequency calculations have been performed based on the density functional theory (DFT) using the DMol3 program [21,22] as a part of Materials Studio package [23]. The results have been obtained for the crystalline state within generalized gradient approximation (GGA) at BLYP (Becke exchange [24] plus Lee–Yang–Parr correction functional [25]) and PW91 functionals, as well as within the local density approximation (LDA) at PWC functional (Perdew–Wang GGA [26]). Calculations have been performed using DNP basis set as implemented in DMol3.

Table 1
Crystal data and structure refinement for 2,5-DMP·CLA adduct.

	2,5-DMP·CLA
Empirical formula	$C_6H_8N_2$ $C_6H_2Cl_2O_4$
Formula weight	317.12
Temperature, K	100(2)
Wavelength (Å)	0.71073
Crystal system	Triclinic
Space group	P-1
Unit cell dimensions	
a (Å)	5.065(1)
b (Å)	8.092(2)
c (Å)	8.952(2)
α (°)	113.86(2)
β (°)	102.04(1)
γ (°)	94.29(1)
Volume (Å^3)	322.93(14)
Z	1
Calculated density, Mg m^{-3}	1.631
μ (mm^{-1})	0.517
Crystal size (mm)	0.40 × 0.12 × 0.10
θ range for data collection (°)	4.18–26.5
Index range	$-6 \leqslant \mathbf{h} \leqslant 6$ $-10 \leqslant \mathbf{k} \leqslant 10$ $-11 \leqslant \mathbf{l} \leqslant 11$
Reflections collected/unique	2188/1341
R_{int}	0.0324
Max and min absorption correction	0.950, 0.829
Data/parameters	1341/96
Goodness-of-fit on F^2	1.093
Final R_1 and wR_2 indices [$I > 2\sigma(I)$]	0.0322, 0.0831
R_1 and wR_2 indices (all data)	0.0396, 0.0858
$\Delta\rho_{max}$, $\Delta\rho_{min}$ (e Å^{-3})	0.246 and −0.258

3. Results and discussion

3.1. X-ray diffraction

The 2,5-DMP CLA adduct crystallizes in the triclinic space group P-1 with only one formula unit per unit cell. The asymmetric unit consists of a half neutral 2,5-DMP molecule and a half neutral CLA molecule. Each molecule in the adduct lies on a crystallographic center of inversion. The structure with atom numbering scheme is shown in Fig. 1.

The selected bond lengths and angles together with the calculated ones for the crystalline state are presented in Table 2. The consistency between corresponding lengths and angles is satisfactory. The rings of 2,5-DMP and CLA lay almost in the same plane. The angle between ring planes equals to merely 5.4(1)°.

The CLA and 2,5-DMP molecules are linked by an intermolecular O–H···N hydrogen-bonding interaction (Fig. 2). Each nitrogen atom of the 2,5-DMP molecule accepts one hydrogen bond from the hydroxyl group of the CLA molecule. The O(4)–H(4)···N(1) distance is indicating a moderate hydrogen bond, with a distance of 2.694(2) Å. The calculated values of the O–H···N bond lengths (2.678 Å) correspond well to the experimental ones. The O(4) atom makes possible a formation of bifurcated hydrogen bonded system, as it is also involved in an intramolecular O(4)–H(4)···O(1) interactions with a distance of 2.699(2) Å.

In the crystal structure of the title adduct, there are two intermolecular C–H···O bridges, which link the 2,5-DMP and CLA moieties into molecular chains extended along the *b*-axis. The chains of the structural units are stabilized through the C–H···O hydrogen bonds. In Table 3 the other short contacts, found in the crystal structure of the 2,5-DMP·CLA complex, are collected.

Of some importance are also bridges formed between aromatic C(16)–H(16) and methyl group C(17)–H(73) bonds with the O(1) and O(4) oxygen atoms of CLA molecule. The corresponding C–H···O distances are equal to 3.030(2) Å and 3.292(2) Å, respectively. The interactions between methyl groups of 2,5-DMP and chlorine atoms of CLA (C(17)–H(71)···Cl(1), 3.935(2) Å) are the factors playing additional role in the linking the chains.

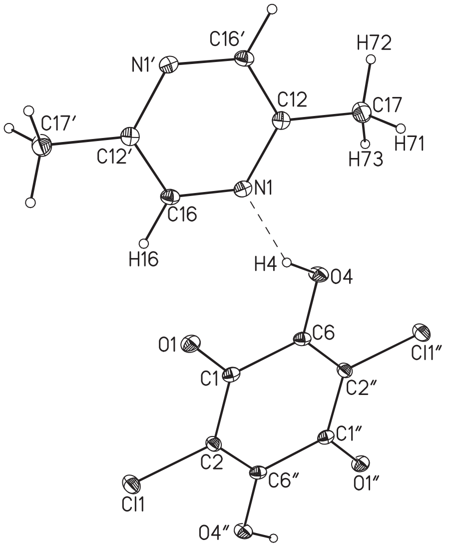

Fig. 1. The structure of 2,5-DMP CLA unit with atom numbering showing displacement ellipsoids at the 30% probability level.

Table 2
Experimental and calculated (by using various models) bond lengths and angles for 2,5-DMP·CLA complex. (Å, °).

Coordinates	Experimental	Calculated		
		PWC(dnp)	PW91(dnp)	BLYP(dnp)
N(1)–C(12)	1.354	1.342	1.350	1.354
C(12)–C(16)''	1.394	1.395	1.398	1.400
C(16)–N(1)	1.333	1.330	1.338	1.343
C(12)–C(17)	1.496	1.477	1.491	1.499
C(1)–O(1)	1.216	1.232	1.236	1.239
C(1)–C(2)	1.470	1.442	1.449	1.452
C(2)–C(6)'	1.348	1.366	1.367	1.368
C(6)–C(1)	1.511	1.497	1.509	1.518
C(6)–O(4)	1.328	1.306	1.320	1.328
C(2)–C(l1)	1.722	1.713	1.730	1.749
C(12)–C(16)''–N(1)''	122.90	122.50	122.63	122.44
C(16)–N(1)–C(12)	117.52	118.25	118.00	118.29
N(1)–C(12)–C(16)''	119.57	119.25	119.36	119.26
C(17)–C(12)–N(1)	118.65	119.34	119.29	119.30
C(17)–C(12)–C(16)''	121.76	121.38	121.32	121.42
C(6)–C(1)–C(2)	118.12	118.89	118.64	118.35
C(1)–C(2)–C(6)'	121.27	121.41	121.37	121.45
C(2)–C(6)–C(1)	120.61	119.70	120.00	120.20
O(1)–C(1)–C(6)	118.51	117.25	117.86	118.09
O(1)–C(1)–C(2)	123.36	123.86	123.60	123.56
O(4)–C(6)–C(2)'	122.32	122.85	122.27	121.99
O(4)–C(6)–C(1)	117.08	117.45	117.74	117.81
Cl(1)–C(2)–C(6)'	121.99	121.61	121.76	121.62
Cl(1)–C(2)–C(1)	116.74	116.98	116.87	116.92

Symmetry code: (') -x, -y, -z; ('') -x, -y, -z.

3.2. Vibrational spectra

3.2.1. Selection rules for the 2,5-DMP·CLA adduct triclinic system, space group P-1, Z = 1

Both 2,5-DMP and CLA molecules occupy C_i sites in the crystal lattice. Formal classification of the fundamental modes ($k = 0$) are listed in Table 4. In the INS spectra all modes are allowed, there is no selection rules related to the symmetry of both a molecule and the crystal structure.

Table 3
Hydrogen bonds and short contacts for 2,5-DMP·CLA adduct.

D–H···A (Å)	D–H (Å)	H···A (Å)	D···A (Å)	<DHN (°)
O(4)–H(4)···N(1)	0.82(2)	1.95(2)	2.694(2)	151(2)
O(4)–H(4)···O(1)	0.82(2)	2.25(2)	2.699(2)	115(2)
C(16)–H(16)···O(1)	0.93	2.39	3.030(2)	126
C(17)–H(73)···O(4)	0.96	2.56	3.292(2)	133
C(17)–H(71)···Cl(1)^{i}	0.96	2.99	3.935(2)	167

Symmetry code: (i) $x + 1$, $y + 1$, $z + 1$.

Table 4
Classification of the fundamental modes[a] for the 2,5-DMP-CLA adduct crystal.

UCG	Lattice modes			Internal modes		Selection rules	
C_i	Ac	Lib	Trans	2,5-DMP	CLA	IR	Raman
A_g	0	6	0	21	18	i	Xx,yy,zz,xy,yz,zx
A_u	3	0	3	21	18	X, Y, Z	i

[a] UCG – Unit cell group; Ac – Acoustic modes, Lib – Librational modes; Trans – Translational modes.

The observed frequencies of particular modes in INS, infra-red and Raman spectra compared with calculated ones are presented in Table 5.

The assignment of particular modes was based on the main contribution derived from the normal coordinate analysis. None of scaling factors was used. As Fig. 3 shows, in infra-red spectra a continuum of absorption spread from *ca.* 3000 cm^{-1} down to *ca.* 500 cm^{-1} is visible with clearly indicated submaxima, the first one between *ca.* 3000 cm^{-1} and 2100 cm^{-1} with maximum at 2400 cm^{-1}, second one rather weak at 1825 cm^{-1} and finally the third one with overlapped narrow peaks of internal modes at *ca.* 1150 cm^{-1}. This picture resembles the Hadži's trio, analyzed in several papers [27]. It indicates a specificity of strong O–H···N hydrogen bond present in our case and may suggest a presence of a double minimum potential for the proton motion.

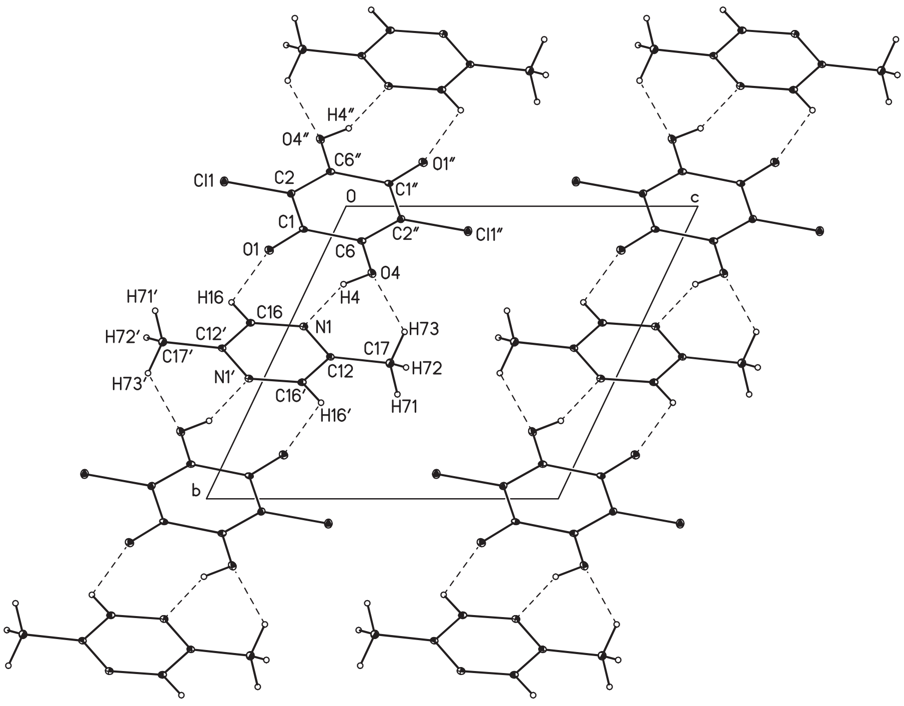

Fig. 2. Packing of the 2,5-DMP and CLA molecules in the crystalline lattice.

Table 5
Experimental and calculated frequencies for 2,5-DMP·CLA complex (cm^{-1}).

Approximate assignments	Experimental				Calculated	
	INS	IR	Raman	PWC(dnp)	PW91(dnp)	BLYP(dnp)
Translation and rotation (9 modes)		78		54–141	67–147	66–145
$CH_{3tors.}$ (25DMP)	51			35	152	148
$CH_{3tors.}$ (25DMP)	51			46	172	155
Ring tors. (CLA)	101	116		118	115	115
Ring tors. (CLA)	130			125	126	132
Ring tors. (25DMP)	165			153	160	164
Ring tors. (CLA)				159	173	174
$C–Cl_{bend.}$ (CLA)	208	202		190	203	202
$C–O_{wagg.}$ (CLA)	226			213	222	217
$C–Cl_{bend.}$ (CLA)			243	231	246	246
$C–O_{bend.}$ (CLA)	294		288	291	292	290
$C–O_{bend.}$ (CLA)		313		305	314	312
$C–Cl_{wagg.}$ (CLA)	322			311	324	318
$C–CH_{3bend.}$ (25DMP)	345	344	337	335	344	346
Ring tors. (25DMP)		357		355	359	355
Ring def. (CLA)			385	386	386	381
$C{=}O_{bend.}$ (CLA)	395	387		396	390	388
Ring def. (CLA)				407	410	408
$C–CH_{3bend.}$ (25DMP)	426	419	418	418	421	423
Ring tors. (25DMP)				419	431	431
$C–O_{wagg.}$ (CLA)		506	496	503	503	499
$C–CH_{3wagg.}$ (25DMP)			513	507	511	513
Ring def. (CLA)		520		512	514	515
$C–Cl_{str.}$(CLA)			528	526	533	531
Ring def. (25DMP)		554		553	553	544
$C–Cl_{wagg.}$ (CLA)		573		583	584	581
Ring def. (25DMP)			676	674	675	681
$C{=}O_{wagg.}$ (CLA)			744	744	749	743
$C–CH_{3str.}$ (25DMP)		746		744	752	744
$C–CH_{3wagg.}$ (25DMP)	751			759	753	750
$C{=}O_{bend.}$ (CLA)				774	774	769
$C{=}O_{wagg.}$ (CLA)		790	785	790	792	785
$C–C_{str.}$ (CLA)		824	832	836	828	809
$C–Cl_{str.}$(CLA)		840		864	869	859
$C–CH_{3\ str.}$ (25DMP)			865	873	899	869
$C–H_{wagg.}$ (25DMP)		890	905	913	900	891
$C–H_{wagg.}$ (25DMP)				923	953	939
$C–C_{str.}$ (CLA)	974			955	982	972
$CH_{3rock.}$ (25DMP)		990		988	995	984
$CH_{3rock.}$ (25DMP)			1014	1001	1021	1027
Ring def. (25DMP)				1002	1029	1042
$CH_{3rock.}$ (25DMP)				1006	1033	1043
$CH_{3\ rock.}$ (25DMP)		1054		1035	1044	1047
$O–H_{wagg.}$ (CLA)				1088	1046	1055
$O–H_{wagg.}$ (CLA)				1090	1046	1055
$O–H_{bend.}$ (CLA)		1153		1112	1172	1182
$C–C_{str.}$(CLA)				1166	1218	1211
$C–C_{str.}$(CLA)				1233	1232	1221
Ring str. (25DMP)		1227		1236	1245	1225
Ring str. (25DMP)			1236	1254	1247	1239
$O–H_{bend.}$ (CLA)				1271	1250	1247
$C–H_{bend.}$ (25DMP)		1261		1281	1266	1253
$C–H_{bend.}$ (25DMP)				1304	1283	1285
$C–O_{str.}$ (CLA)			1302	1329	1333	1302
$C–O_{str.}$ (CLA)			1332	1345	1342	1308
Ring str. (25DMP)		1365		1358	1364	1357
$CH_{3bend.}$ (25DMP)		1404	1393	1360	1374	1396
$CH_{3bend.}$ (25DMP)				1376	1388	1406
$CH_{3bend.}$ (25DMP)		1455		1389	1442	1453
$CH_{3bend.}$ (25DMP)		1459		1397	1447	1455
$CH_{3bend.}$ (25DMP)		1465		1398	1449	1463
Ring str. (25DMP)		1489		1421	1464	1474
$CH_{3bend.}$ (25DMP)		1494		1484	1476	1482
Ring str. (25DMP)		1539		1564	1540	1520
$C{=}C_{str.}$ (CLA)		1550		1604	1596	1579
Ring str. (25DMP)				1623	1608	1591
$C{=}C_{str.}$ (CLA)		1622		1629	1634	1604
$C{=}O_{str.}$ (CLA)			1630	1672	1654	1629
$C{=}O_{str.}$ (CLA)			1634	1674	1655	1629
$O–H\cdots N_{str.}$		~2500		2311	2510	2518
$O–H\cdots N_{str.}$		~2500		2345	2542	2551
$C_m–H_{str.}$			2923	2944	3016	3013
$C_m–H_{str.}$				2944	3016	3014
$C–H_{str.}$			3076	3027	3103	3081

(*continued on next page*)

Table 5 (*continued*)

Approximate assignments	Experimental				Calculated	
	INS	IR	Raman	PWC(dnp)	PW91(dnp)	BLYP(dnp)
C–$H_{str.}$				3027	3103	3082
C_m–$H_{str.}$				3070	3147	3123
C_m–$H_{str.}$				3071	3148	3125
C_m–$H_{str.}$				3105	3166	3195
C_m–$H_{str.}$				3106	3167	3196

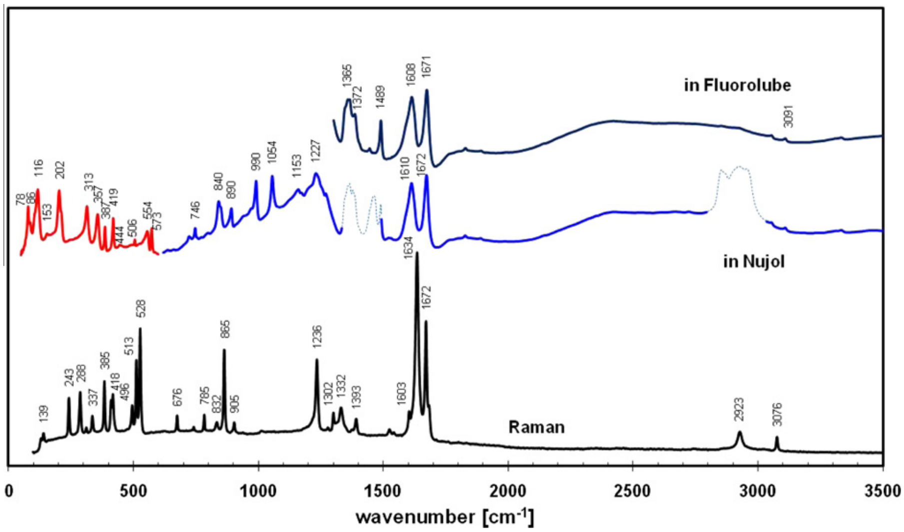

Fig. 3. Comparison of the infra-red and Raman spectra in the wavenumber range between 100 and 3500 cm^{-1}. The absorption arising from Nujol is shown as dotted line.

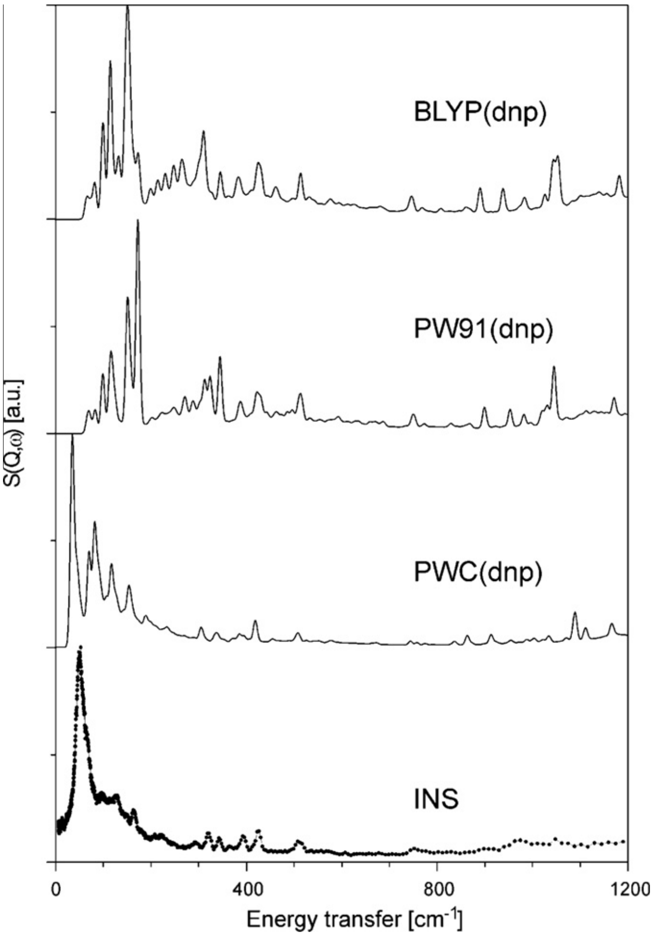

Fig. 4. The INS spectrum confronted with simulated ones by using various models.

The comparison of the infra-red and Raman spectra in the medium frequency range is shown in Fig. 3 as well, allowing a possibility of quantitative comparison of observed peaks.

The INS spectrum, in the frequency range up to 1200 cm^{-1}, compared with simulated ones by using various models merits a special treatment (Fig. 4).

The experimental spectrum shows particularly strong band at 51 cm^{-1}, which should be ascribed to the torsional/librational vibrations of methyl groups. The best reproduction is obtained by using the PWC functional. Remaining two other PW91 and BLYP models lead to very high frequencies of CH_3 torsional mode, three times as high as experimental values. In the case of the other modes all three models yield highly similar frequencies.

4. Conclusions

The 2,5-DMP and CLA molecules form in the crystalline lattice the infinite equivalent hydrogen bonded chains with the O–H···N length equal to 2.694(2) Å. These strong bridges find a reflection in the infrared continua that suggest a double minimum potential in the excited vibrational state. According to the Zundel's theory [28] such bridges are characterized by a very high polarizability and as a consequence by the unusual width of stretching vibrational bands. In addition to the O–H···N hydrogen bonds the bifurcate O–H···O bridges, strongly bent, are present.

The origin of a trio on the broad continuous absorption can be explained as due to the splitting of the energetic levels in the excited vibrational state. Simultaneously one should take into account the coupling with the overtone of the C–$H_{wagg.}$ mode that leads to a creation of an Evans hole on the absorption curve and an appearance of the pseudoband located at 1825 cm^{-1}.

In the present paper we did not analyze the behavior of hydrogen bonds with the participation of the C–H groups. Here we want to tell that analogous features of the C–H groups engaged into

C–H···Y hydrogen bonds were analyzed in the complex of 2,6-dimethylpyrazine with CLA [17]. The results in this case show that the aromatic C–H groups form the connections with a weak red-shifting effect. In a case of the methyl groups we observe quite well the blue-shifting so that the improper hydrogen bonds.

The analysis of the structure and vibrational modes has been performed by using three different models applied to the crystalline state. Both the calculated structure and the mode frequencies are well consistent, except the CH_3 torsional mode. Relatively good agreement was achieved only by using the PWC functional.

Acknowledgments

The calculations were performed on computers of the Wroclaw Centre for Networking and Supercomputing, under Calculating Grant No. 2006/5, and in Interdisciplinary Centre for Mathematical and Computational Modeling, Warsaw University, under Calculating Grant No. G30-15. MATERIALS STUDIO package was used under POLAND COUNTRY-WIDE LICENSE.

This work was supported by the Polish Ministry of Science and Higher Education (Project Register No. N N204 2497 34).

References

[1] H. Ishida, S. Kashino, Acta Cryst. C55 (1999) 1714.
[2] A.M. Kutasi, S.R. Batten, A.R. Harris, B. Moubaraki, K.S. Murray, Aust. J. Chem. 55 (2002) 311.
[3] F.B. Abrahams, S.R. Batten, B.F. Hoskins, R. Robson, Inorg. Chem. 42 (2003) 2654.
[4] S.R. Batten, B.F. Hoskins, B. Moubaraki, K.S. Murray, R. Robson, Cryst. Eng. Commun. (2001) 8.
[5] L. Brammer, M.D. Burgard, C.S. Rodger, J.K. Swearingen, K. John, N.P. Rath, Chem. Commun. (2001) 2468.
[6] M.d.B. Zaman, M. Tomura, Y. Yamashita, Chem. Commun. (1999) 999.
[7] M.d.B. Zaman, M. Tomura, Y. Yamashita, J. Org. Chem. 66 (2001) 5987.
[8] G. Gilli, V. Bertolasi, P. Gilli, V. Forretti, Acta Cryst. B57 (2001) 859.
[9] J.B. Clinman, M. David, Ann. Rev. Biochem. 63 (1994) 299.
[10] M. Prager, A. Pawlukojć, L. Sobczyk, E. Grech, H. Grimm, J. Phys.: Condens. Matter 17 (2005) 5725.
[11] M. Prager, A. Pietraszko, L. Sobczyk, A. Pawlukojć, E. Grech, T. Seydel, A. Wischnewski, M. Zamponi, J. Chem. Phys. 125 (2006) 194525.
[12] J. Nowicka-Scheibe, E. Grech, W. Sawka-Dobrowolska, G. Bator, L. Sobczyk, Polish J. Chem. 81 (2007) 643.
[13] M. Prager, A. Wischnewski, G. Bator, E. Grech, A. Pawlukojć, L. Sobczyk, Chem. Phys. 334 (2007) 148.
[14] X.-Q. Cai, M.-L. Hu, Y.-J. Zhao, Y.-O. Cheng, S. Wang, Acta Cryst. E61 (2005) 614.
[15] A. Pawlukojć, W. Sawka-Dobrowolska, G. Bator, L. Sobczyk, E. Grech, J. Nowicka- Scheibe, J. Wuttke, J. Mol. Struct. (2010). Available from: <http://dx.doi.org/10.1016/j.molstruc.2010.04.041>.
[16] M. Prager, W. Sawka-Dobrowolska, L. Sobczyk, A. Pawlukojć, E. Grech, A. Wischnewski, M. Zamponi, Chem. Phys. 332 (2007) 1.
[17] A. Pawlukojć, L. Sobczyk, M. Prager, A. Bator, E. Grech, J. Nowicka-Scheibe, J. Mol. Struct. 892 (2008) 261.
[18] J.F. Arenas, J.T. Lopez-Navarrete, J.I. Marcos, J.C. Otero, J. Mol. Struct. 162 (1987) 263.
[19] G.M. Sheldrick, SHELXL-97, Program for Solution of Crystal Structure, University of Göttingen, Germany, 1997.
[20] I. Natkaniec, S.I. Bragin, I. Brankowski, J. Mayer, in: Proc. ICANS XIII, Abington, RAL Report 94-025, vol. I, 1993, p. 89.
[21] B. Dalley, J. Chem. Phys. 92 (1990) 508.
[22] B. Dalley, J. Chem. Phys. 113 (2000) 7756.
[23] <http://www.accelrys.com/>.
[24] A.D. Becke, J. Chem. Phys. 88 (1988) 2547.
[25] C. Lee, W. Yang, R.G. Parr, Phys. Rev. B37 (1988) 785.
[26] J.P. Perdew, Y. Wang, Phys. Rev. B45 (1992) 13244.
[27] D. Hadži, S. Bratos, Vibrational spectroscopy of the hydrogen bond, in: P. Schuster, G. Zundel, C. Sandorfy (Eds.), The Hydrogen Bond, Structure and Spectroscopy, vol. II, North-Holland, Amsterdam, Newyork, Oxford, 1976, p. 565.
[28] G. Zundel, Adv. Chem. Phys. 111 (2000) 1.